Journal of Engineering Mathematics, Vol. 13, No. 4, October 1979
© 1979 Sijthoff & Noordhoff International Publishers – Alphen aan den Rijn
Printed in the Netherlands

# On the optimization of the thrust of a yacht sailing to windward

A. K. WIERSMA

*Department of Mathematics, University of Groningen, Groningen, The Netherlands*

(Received May 17, 1979)

SUMMARY

Constraints are put on the heeling moment and on the distribution of forces over mainsail, foresail, keel and rudder. A linear theory is developed by which the influence of these constraints on optimum spanwise circulation distributions can be calculated. The air and the water are considered to be incompressible. Allowance is made for the dependence of the wind velocity on the height above the watersurface.

## 1. Introduction

A sailing yacht moves at the boundary of two media, air and water, which have a different velocity in any chosen coordinate system. When sailing to windward, which will be discussed in this paper, a driving force is developed by exchanging momentum between the two media. For the description of the force production we use a linearized lifting-surface theory. It is clear that when we neglect the influence of the mast, the sails can be considered as lifting surfaces without thickness. The action of the underwater part of the yacht (hull, keel plus rudder), which we will call the underwatership, is described by also considering it as a flat lifting surface of zero thickness. It terminates at the water surface which is assumed to be rigid and flat, so we leave aside the wavemaking. We hope that this mathematical model is not too crude to describe some aspects of the hydro- and aerodynamic action of the yacht.

The thrust is needed to overcome the various kinds of resistance experienced by the yacht. There are the frictional and form resistance of sails, rigging, hull and underwatership and the wave resistance. Furthermore there is the induced resistance which is inherent in force production by lifting surfaces of finite span. Since induced resistance depends on the spanwise circulation distributions of sails and keel, and hence on their form, it can be minimized under certain constraints on lift and heeling moment. This optimization problem is tackled in this paper.

In Fig. 1.1 we have drawn schematically the sails and the underwatership in a coordinate system fixed to the yacht. The sails have deviations of $O(\epsilon)$ from surfaces which would not disturb the incoming air velocity ($U$), which makes an angle $\alpha$ with the yacht's centreline $C_L$. The centreline is defined as the intersection of the longitudinal plane of symmetry with the watersurface, and it is assumed to be a fixed line with respect to the yacht. (We introduced here the linearization parameter $\epsilon$, whose magnitude hence is determined by the camber and local angles of attack of the sails). In order that the underwatership is able to act as a lifting surface and to prevent

flow separation, the angle $\lambda$ between $C_L$ and the undisturbed water velocity $V$ must be small (we assume it to be of order $\epsilon$); $\lambda$ is called the leeway angle.
The induced resistances of sails and underwatership are of comparable magnitude. In his well-known book [2], Juan Baader makes a rough estimate of the air resistance (with the exception of the induced resistance) of hull, rigging and sails of a Dragon yacht. He shows that, when sailing close to wind, this resistance becomes of the order of magnitude of the frictional resistance of the underwatership. Now, because the wave resistance acts in the direction of $V$, the total resistance will have a direction which is closer to $V$ than to $U$. Then it is easily seen that the sails contribute more to the driving force than the underwatership. Therefore $\alpha$ can not be too small (sailing practice shows that in general $\alpha \gtrsim 20$). For the rest there is no fundamental difference between the hydrodynamic action of the underwatership and the aerodynamic action of the sails. We remark that the total force perpendicular to the total resistance must be zero.

We will consider situations where $\alpha$ is $O(\epsilon^\circ)$. The situations where $\alpha$ can be assumed to be $O(\epsilon)$ (perhaps $20^\circ \leq \alpha \leq 35^\circ$) are discussed in [8]. In general we prescribe the total sideforce experienced by fore- and mainsail. However, because the free vortex sheets of fore- and mainsail do not coincide in our linearized theory, the induced resistance will depend on the way both sails contribute to the total sideforce. It can be useful to prescribe the sideforces of fore- and mainsail separately, for example when their areas differ substantially. So we will prescribe these sideforces separately and furthermore the total heeling moment around the yacht's centreline. Under these constraints the induced resistance is minimized. The same problem can be formulated for the single lifting surface representing the underwatership. This has already been discussed in [6]. The two systems of lifting surfaces are coupled and the combined second-order thrust is optimized under the constraint of zero total sideforce and heeling moment, given the righting moment of the yacht as a function of the heeling angle.

The water and air will be nonviscous and incompressible. The water will have a uniform velocity. Milgram [4] approximately took into account the variation of the wind velocity with height above the water surface. Here we will consider a velocity profile consisting of a uniform part of $O(\epsilon^\circ)$ plus a part of $O(\epsilon)$ which depends on the height above the watersurface. This seems not unrealistic when we consider for example the velocity profile given by Marchaj ([3], fig. 238), taking into account the fact that by the yacht's velocity the apparent wind has a still larger uniform part.

At least two objections against the proposed optimization problem can be made. In the first place not all forces of $O(\epsilon^2)$, which contribute to the thrust, can be taken into account in a linearized theory. This will be discussed in the next section. Secondly we prescribe a sideforce, and hence also a thrust of $O(\epsilon)$. Hence one may wonder what is the use of optimizing the $O(\epsilon^2)$ contribution to the thrust, since theoretically we can give the sideforce every value of $O(\epsilon)$. Then we can obtain every required thrust by making the sideforce large enough without bothering about the $O(\epsilon^2)$ part of the thrust. In practice, however, there are limits to the forces which can be generated by lifting surfaces. This will be discussed in the numerical section.

The shortcomings of the mathematical model used to describe the flow around the sails have been discussed extensively by Wood and Tan [9].

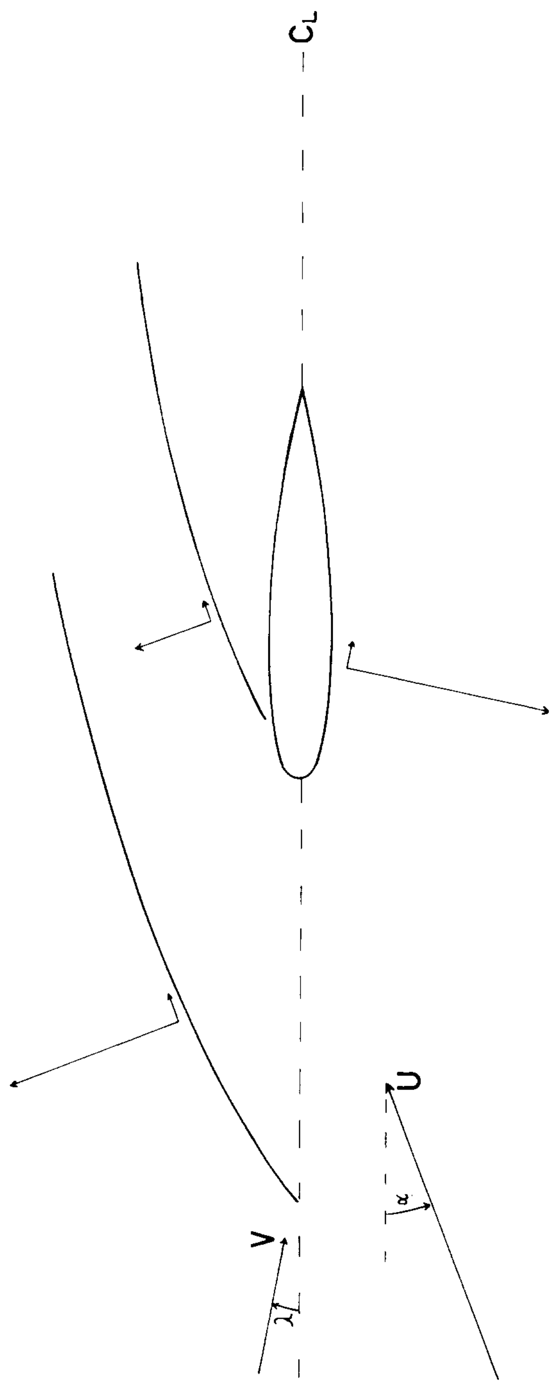


Fig. 1.1 Forces acting on the sails and the underwatership.

## 2. On the $O(\epsilon^2)$ contribution to the thrust of the forces generated by the sails

In our linearized theory we prescribe lift forces and a heeling moment of $O(\epsilon)$. For the sails this means that generally we also prescribe the $O(\epsilon)$ part of the driving force (see Fig. 1.1). Forces and moments of this order of magnitude can be thought to be generated by spanwise circulation distributions of $O(\epsilon)$ of fore- and mainsail ($\Gamma_f$ and $\Gamma_m$ respectively) which are placed in a uniform flow of $O(\epsilon^0)$. The free-vortex sheets of fore- and mainsail induce velocities of $O(\epsilon)$ and besides these there are the velocities of $O(\epsilon)$ from the non-uniform part of the wind. Together these velocities of $O(\epsilon)$ cause a force contribution to the thrust of $O(\epsilon^2)$. This contribution can be optimized by choosing the appropriate spanwise circulation distribution. The optimum circulation distribution can be realized in many ways by designing sails which have the proper deviations (of $O(\epsilon)$) from surfaces which do not disturb the air. In general, however, the asymptotic expansion in the parameter $\epsilon$ of the lift produced by the sails will have a non-zero term of $O(\epsilon^2)$. Hence there will be another contribution of $O(\epsilon^2)$ to the driving force, about which no exact information is supplied by a linearized theory. And up to now only in a linearized theory we can perform the mentioned optimization.

We observe here that there is evidence that a single lifting surface, described by $z = c_1 + \epsilon f_1(x,y)$, $((x,y) \in S_1, f_1(x,y)$ of $O(\epsilon^0)$, Fig. 2.1), which is placed in an unbounded medium, misses the $O(\epsilon^2)$ term in the asymptotic expansion of its lift $L$.
For, suppose the exact lift $L$ has an expansion $L(\epsilon) = \epsilon L_1 + \epsilon^2 L_2 + \epsilon^3 L_3 + \epsilon^4 L_4 + \dots$ . Now we change the sign of $\epsilon$, then the new lift becomes $L(-\epsilon) = -\epsilon L_1 + \epsilon^2 L_2 - \epsilon^3 L_3 + \epsilon^4 L_4 - \dots$ . It is easy to see that $L(\epsilon) = -L(-\epsilon)$ and hence $L_2 = L_4 = \dots = 0$. In this context we also refer to Ashley and Landahl ([1], pp. 135-136). Now when a second lifting surface ($z = c_2 + \epsilon f_2(x,y)$, $(x,y), \in S_2$) is added generally the identity $L(-\epsilon) = -L(\epsilon)$ does not hold anymore. From these considerations we can cautiously make the presumption that the occurrence of an $O(\epsilon^2)$ term in the lift is typically due to the interaction of the sails. Anyway its strength will depend on the chordwise pressure distributions along the sails.

Now, given a spanwise circulation distribution, we can choose chordwise pressure distributions which optimize the $O(\epsilon^2)$ term in the lift. Then there remains the question whether the optimum *spanwise* circulation distribution may have an adverse effect on the $O(\epsilon^2)$ term in the lift of the

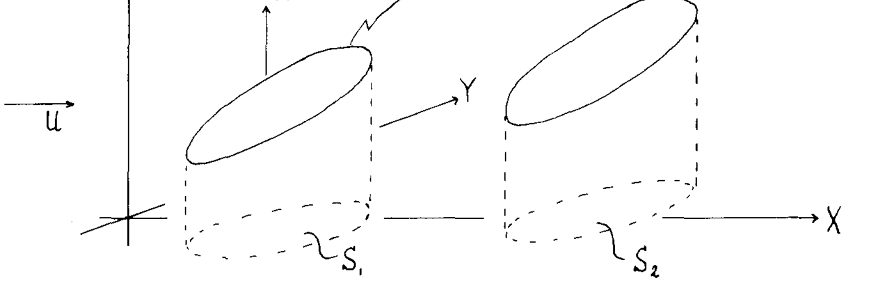


Fig. 2.1

sails, or stated otherwise: are there non-optimum *spanwise* circulation distributions which, with the proper *chordwise* pressure distributions, will enlarge the *total* $O(\epsilon^2)$ contribution to the thrust. Unfortunately we cannot answer this question. However, we hope that the contributions of $O(\epsilon^2)$ to the thrust which we take into account in the optimization process are dominant, so that it makes sense to optimize them.

Finally we remark that when the yacht heels over a finite angle these considerations also apply to the single lifting surface representing the underwatership, because the rigid and flat water-surface acts as a mirror. Then the reflection of the underwatership forms the second lifting surface.

## 3. Statement of the problem for the sails

Consider a right-handed coordinate system $\bar{X},\bar{Y},\bar{Z}$, at rest with respect to the undisturbed water. The $\bar{X},\bar{Y}$-plane coincides with the watersurface which is assumed to be rigid and flat. The undisturbed air has a velocity $U(\bar{z})$ which makes an angle $\bar{\alpha}^*$ with the $\bar{X},\bar{Z}$-plane. Its magnitude depends upon the height above the watersurface:

$$U(\bar{z}) = U_0^* + \bar{f}^*(\bar{z}). \tag{3.1}$$

We assume that $\bar{f}^*(\bar{z})$ is of order $\epsilon$, where the linearization parameter $\epsilon$ is defined by the shape of the sails as is done for instance in Fig. 2.1.

We will restrict ourselves to yachts with one mast, where the foresail is guided along the forestay which ends at the top of the mast. The centreline $C_L$ of the yacht is parallel to the $\bar{X}$-axis. In Fig. 3.1 the foot of the mast just has arrived at the origin of our coordinate system, hence $C_L$ coincides with the $\bar{X}$-axis. The yacht heels, making an angle $\beta$ with the $\bar{X},\bar{Y}$-plane. It will have a velocity $V$ of $O(\epsilon^0)$ in the negative $\bar{X}$-direction. Furthermore it has a velocity $\lambda V$ of $O(\epsilon)$ in positive $\bar{Y}$-direction. $\lambda$ is the small leeway angle, which we assume to be of $O(\epsilon)$.

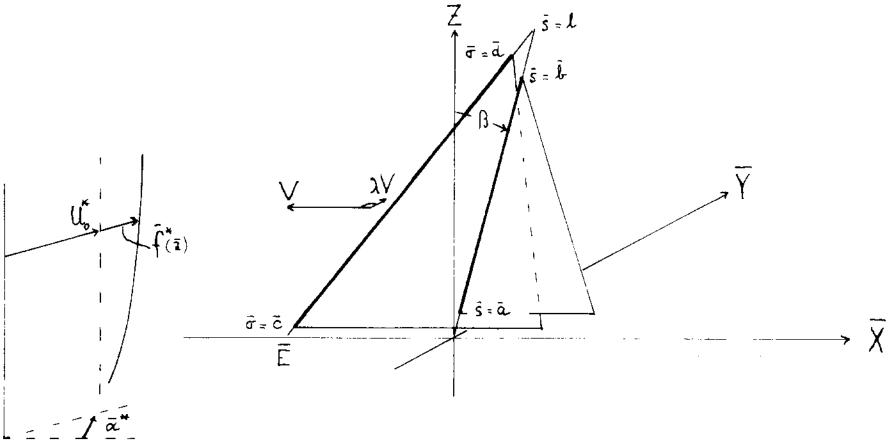


Fig. 3.1 The 'physical' coordinate system.

The sails will cause disturbance velocities of $O(\epsilon)$. In an unpublished note Sparenberg [5] remarks that the $O(\epsilon)$ part of the velocity of the undisturbed air $(\bar{f}^*(\bar{z}), (3.1))$ drops out of the linearized equations of motion and the continuity equation. Hence, although the incoming air has continuously distributed vorticity of order $\epsilon$, we can use the concept of free vorticity shed by the sails. The function $\bar{f}^*(\bar{z})$ enters, however, in the optimization problem and therefore it influences the optimum circulation distribution.

In this paper we are interested in optimum spanwise circulation distributions under certain constraints on sideforce and heeling moment. Hence we may, since we use a linearized theory, without restricting generality replace the sails by lifting lines (abbreviated by l.l's). The l.l. representing the mainsail is chosen along the mast extending from $\bar{s} = \bar{a}$ to $\bar{s} = \bar{b}$, where $\bar{s}$ is a length parameter denoting the distance to the $\bar{X}$-axis. The l.l. representing the foresail coincides with a part of the forestay and extends from $\bar{\sigma} = \bar{c}$ to $\bar{\sigma} = \bar{d}$. Here $\bar{\sigma}$ denotes the distance to the point of attachment $\bar{E}$ of the forestay at the deck. $\bar{E}$ has the coordinates $(-\bar{e}, 0, 0)$. The angle between forestay and mast is $\gamma$.

The crew on board the yacht will feel the apparent wind. The $O(\epsilon^0)$ part $\mathbf{U}_0$ of this apparent wind has the magnitude

$$U_0 = |\mathbf{U}_0| = (U_0^{*2} + V^2 + 2U_0^* V \cos \bar{\alpha}^*)^{\frac{1}{2}} \tag{3.2}$$

and it makes an angle $\alpha$ with the $\bar{X}$-axis:

$$\alpha = \text{arctg} \frac{U_0^* \sin \bar{\alpha}^*}{U_0^* \cos \bar{\alpha}^* + V}. \tag{3.3}$$

The $O(\epsilon)$ part of the apparent wind, called $\bar{\mathbf{f}}(\bar{z})$ has a strength

$$\bar{f}(\bar{z}) = |\bar{\mathbf{f}}(\bar{z})| = \{\bar{f}^{*2}(\bar{z}) + \lambda^2 V^2 - 2\lambda V \bar{f}^*(\bar{z}) \sin \bar{\alpha}^*\}^{\frac{1}{2}} \tag{3.4}$$

and it makes an angle $\bar{\alpha}$ with the $\bar{X}$-axis:

$$\bar{\alpha} = \text{arctg} \frac{\bar{f}^*(\bar{z}) \sin \bar{\alpha}^* - \lambda V}{\bar{f}^*(\bar{z}) \cos \bar{\alpha}^*} . \tag{3.5}$$

We remark that the direction of $\bar{\mathbf{f}}(\bar{z})$ depends on $\bar{z}$ and differs from the direction of $\mathbf{U}_0$ in general.

In order to obtain dimensionless formulae we divide velocities by $U_0$, (3.2), and lengths by $\ell$, where $\ell$ is the height of the mast. Furthermore we introduce a new right-handed coordinate system $X,Y,Z$ which translates with respect to the old system with a velocity $\mathbf{U}_0$ and whose $X$-axis is in the direction of $\mathbf{U}_0$ (Fig. 3.2). In this coordinate system, lengths and velocities are nondimensional and we will use the same symbols as in Fig. 3.1, however we omit all bars, except the one of the angle $\bar{\alpha}$, (3.5). The $X,Y$-plane again coincides with the watersurface. By the choice of $X,Y,Z$ the yacht moves with a velocity of magnitude 1 in the negative $X$-direction, while its centreline $C_L$ makes an angle $\alpha$, (3.3), with the $X$-axis. In the $X,Y,Z$-system the yacht has a velocity $\lambda V$ of $O(\epsilon)$ in the $Y$-direction. In our linearized theory it is consistently taken into

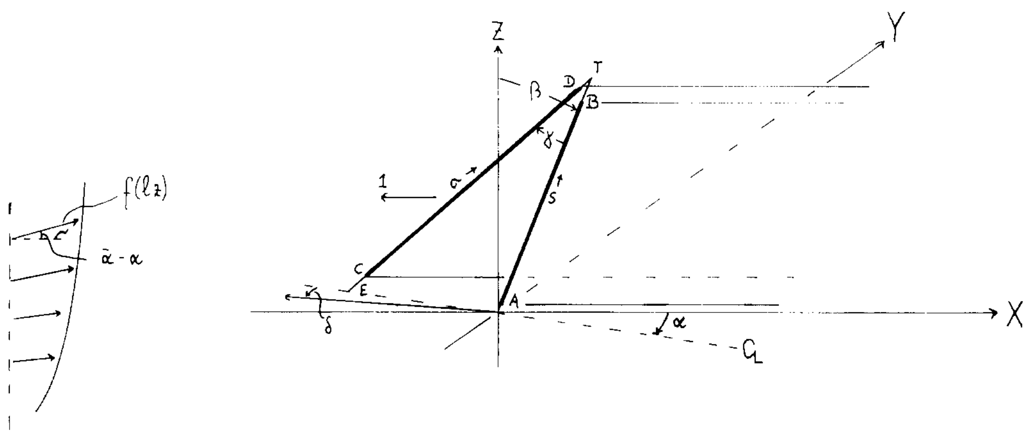


Fig. 3.2 The 'dimensionless' coordinate system X, Y, Z.

account in the system $X,Y,Z$ if we consider also the $O(\epsilon)$ part of the apparent wind in this system. It has a strength $f(\ell z)$ $(=\overline{f(z)}/U_0$, (3.4)) and its $x$-, $y$- and $z$-components are

$$(f(\ell z)\cos(\bar{\alpha}-\alpha),\ \ f(\ell_z)\sin(\bar{\alpha}-\alpha),\ \ 0) \tag{3.6}$$

The coordinates of the points $A$, $B$, $C$, $D$, $E$ and $T$ are

$$\begin{aligned}
A &= (a\sin\beta\sin\alpha, a\sin\beta\cos\alpha, a\cos\beta),\\
B &= (b\sin\beta\sin\alpha, b\sin\beta\cos\alpha, b\cos\beta),\\
C &= ((-e+c\sin\gamma)\cos\alpha + c\cos\gamma\sin\beta\sin\alpha, (e-c\sin\gamma)\sin\alpha +\\
&\qquad\qquad c\cos\gamma\sin\beta\cos\alpha, c\cos\gamma\cos\beta),\\
D &= ((-e+d\sin\gamma)\cos\alpha + d\cos\gamma\sin\beta\sin\alpha, (-e+d\sin\gamma)\sin\alpha +\\
&\qquad\qquad d\cos\gamma\cos\beta\cos\alpha, d\cos\gamma\cos\beta),\\
E &= (-e\cos\alpha, e\sin\alpha, 0),\\
T &= (\sin\beta\sin\alpha, \sin\beta\cos\alpha, \cos\beta).
\end{aligned} \tag{3.7}$$

On their way through the air the l.l.'s leave behind free-vortex sheets which remain on the place where they are shed except for small displacements of $O(\epsilon)$ which however cause errors of $O(\epsilon^2)$ in the induced velocities. The influence of these errors upon lift and induced resistance is of $O(\epsilon^3)$ and can be therefore be neglected. For $x\to\infty$ the direct influence of the 1.1.'s vanishes and the velocity induced by the free-vortex sheets will only have components in $y$- and $z$-direction. The induced velocity q possesses for $x\to\infty$ a dimensionless potential $\varphi=\varphi(y,z)$ which vanishes together with its partial derivatives for $y^2+z^2\to\infty$:

$$\mathrm{q}=(0,q_y,q_z)=\left[0,\frac{\partial\varphi}{\partial y},\frac{\partial\varphi}{\partial z}\right]\ ;\ \varphi,\frac{\partial\varphi}{\partial y},\frac{\partial\varphi}{\partial z}\to 0\ \ \text{for } y^2+z^2\to\infty. \tag{3.8}$$

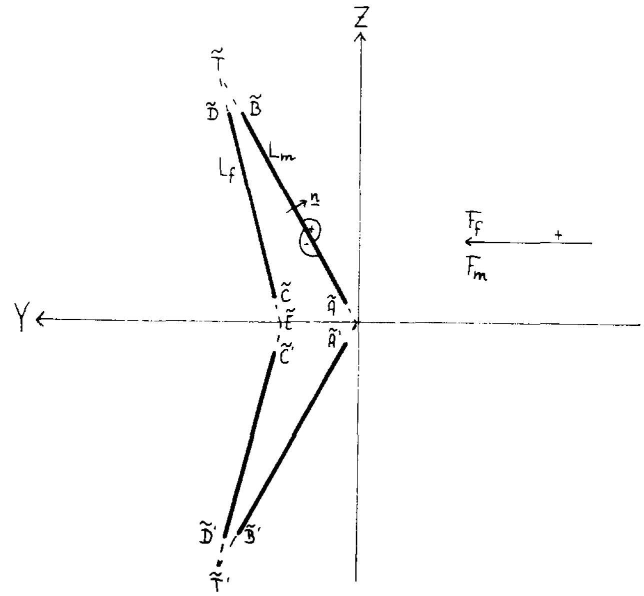


Fig. 3.3 Lines of discontinuity for $\varphi$ in a plane X = constant, far behind the lifting lines.

When passing through the free-vortex sheets the function $\varphi$ has a discontinuity. Further it satisfies Laplace's equation $\Delta\varphi = 0$ everywhere in planes far behind the l.l.'s and perpendicular to the $X$-axis. This implies that the circulation around each free-vortex sheet separately has to be zero.

The cuts formed in the $Y,Z$-plane by the free-vortex sheets of fore- and mainsail are called $L_f$ and $L_m$ respectively. In Fig. 3.3 we have indicated $a$ + - and $a$ – side on these cuts. The coordinates of $\tilde{A}, \tilde{B}, \ldots, \tilde{T}$ are the $y$- and $z$-coordinates of $A, B, \ldots T$, (3.7).
In the plane $z = 0$ (the watersurface) we have the boundary condition of zero normal velocity. In order to satisfy this condition automatically in the following analysis we assume the whole space to be filled with air. Furthermore we introduce the reflection with respect to the $X,Y$-plane of the l.l.'s, their free-vortex sheets and the velocity profile $f(\ell z)$ of the $O(\epsilon)$ part of the apparent wind. We will agree that from now on in our analysis and calculations we will take into account the reflection of all these quantities.

Now let us consider the forces of $O(\epsilon^2)$ which we can calculate and which can contribute to the thrust. First there is the induced resistance $R_i$, acting in positive $X$-direction:

$$R_i = \tfrac{1}{2}\rho U_0^2 \ell^2 \left\{ \int_{L_f} [\varphi]_+^- \frac{\partial\varphi}{\partial n}\, d\tilde{\sigma} + \int_{L_m} [\varphi]_+^- \frac{\partial\varphi}{\partial n}\, d\tilde{s} \right\}. \tag{3.9}$$

Here $\tilde{\sigma}$ and $\tilde{s}$ are length parameters along $L_f$ and $L_m$ giving the distance to $\tilde{E}$ and the $X$-axis respectively (Fig. 3.3.). By $[\varphi]_+^-$ we mean the jump of $\varphi$ over $L_f$ or $L_m$ and $\partial/\partial n$ means differentiation in the direction of the normal on $L_f$ or $L_m$, which points from the – to the + side.

Furthermore there is the force experienced by the l.l.'s on their way through the $O(\epsilon)$-part of the apparent wind (3.4). This force, called $K$, has $x$- and $y$-components $K_x$ (positive in negative $X$-direction) and $K_y$ (positive in positive $Y$-direction):

$$K_x = \rho U_0^2 \ell^2 \cos\beta \left\{ k_f \int_{L_f} f(\ell k_f \cos\beta\tilde{\sigma}) \sin(\bar{\alpha} - \alpha) [\varphi]_+^- d\tilde{\sigma} + k_m \int_{L_m} f(\ell k_m \cos\beta\tilde{s}) \sin(\bar{\alpha} - \alpha) [\varphi]_+^- d\tilde{s} \right\},$$

$$K_y = \rho U_0^2 \ell^2 \cos\beta \left\{ k_f \int_{L_f} f(\ell k_f \cos\beta\tilde{\sigma}) \cos(\bar{\alpha} - \alpha) [\varphi]_+^- d\tilde{\sigma} + k_m \int_{L_m} f(\ell k_m \cos\beta\tilde{s}) \cos(\bar{\alpha} - \alpha) [\varphi]_+^- d\tilde{s} \right\} \tag{3.10}$$

where

$$k_f = \{\cos^2\beta + (\sin\beta\cos\alpha - e\sin\alpha)^2\}^{\frac{1}{2}}, \qquad k_m = \{\cos^2\beta + \sin^2\beta\cos^2\alpha\}^{\frac{1}{2}}. \tag{3.11}$$

We emphasize that on infinitesimal elements of the l.l.'s this aerodynamic force is perpendicular to (3.6) and hence its local direction depends upon the height above the watersurface.

We prescribe the $O(\epsilon)$ part of the aerodynamic sideforces experienced by the fore- and mainsail separately and the $O(\epsilon)$ part of their combined heeling moment. The sideforces are the forces in $Y$-direction, positive in positive $Y$-direction. When the prescribed sideforces on fore- and mainsail are $F_f$ and $F_m$ respectively, we have the following constraints on $\varphi$:

$$F_1(\varphi) \equiv \rho\, U_0^2\, \ell^2 \cos\beta\, k_f \int_{L_f} [\varphi]_+^- d\tilde{\sigma} = F_f, \tag{3.12}$$

$$F_2(\varphi) \equiv \rho\, U_0^2\, \ell^2 \cos\beta\, k_m \int_{L_m} [\varphi]_+^- d\tilde{s} = F_m. \tag{3.13}$$

The heeling moment is the moment around the yacht's centreline, positive if it makes the yacht heel towards the positive $Y$-axis. Its prescribed magnitude is $M_h$, so $\varphi$ also has to satisfy

$$M(\varphi) \equiv \rho\, U_0^2\, \ell^3 \cos\alpha \left\{ \int_{L_f} m(\tilde{\sigma}) [\varphi]_+^- d\tilde{\sigma} + \int_{L_m} \tilde{s} [\varphi]_+^- d\tilde{s} \right\} = M_h, \tag{3.14}$$

where $m(\tilde{\sigma}) = \tilde{\sigma} + e\, k_f \sin\alpha(\sin\beta\cos\alpha - e\sin\alpha)$.

## 4. The optimization problem for the sails

We want to optimize the $O(\epsilon^2)$ contribution to the thrust of the terms given in (3.9) and (3.10). The direction of the thrust makes a prescribed angle $\delta$ with the yacht's centreline (Fig. 3.2), hence we have to optimize the functional $G(\varphi)$.

$$G(\varphi) \equiv K_x \cos(\alpha - \delta) + K_y \sin(\alpha - \delta) - R_i \cos(\alpha - \delta). \tag{4.1}$$

The angle $\delta$ is determined by the total resistance experienced by the yacht. This resistance cannot be calculated in the mathematical model we use, so $\delta$ is one of the parameters of the problem.

In (3.12), (3.13) and (3.14) we gave the constraints which have to be imposed on $\varphi$. Therefore we can introduce the Lagrange multipliers $\lambda_f \cos(\alpha - \delta)$, $\lambda_m \cos(\alpha - \delta)$ and $\lambda_h \ell^{-1} \cos\beta \cos(\alpha - \delta)$ and solve the equivalent problem of optimizing the functional $J(\varphi)$,

$$J(\varphi) = G(\varphi) + \lambda_f \cos(\alpha - \delta) F_1(\varphi) + \lambda_m \cos(\alpha - \delta) F_2(\varphi) + \lambda_h \ell^{-1} \cos\beta \cos(\alpha - \delta) M(\varphi) \tag{4.2}$$

still subject to the constraints (3.12) - (3.14).

A necessary condition for $J$ to have an extreme for some $\varphi$ is that the first variation of $J$ with respect to this $\varphi(\delta J(\varphi))$ vanishes. This yields the relation

$$\begin{aligned}
\delta J(\varphi) = \rho U_0^2 \ell^2 & \int_{L_f} [\delta\varphi]_+^- \Big\{ k_f \cos\beta f(\ell k_f \cos\beta \tilde{\sigma}) \sin(\bar{\alpha} - \delta) + \\
& \cos(\alpha - \delta) \left( \lambda_f k_f \cos\beta + \lambda_h \cos\beta \cos\alpha\, m(\tilde{\sigma}) - \frac{\partial\varphi}{\partial n} \right) \Big\} \, d\tilde{\sigma} + \\
\rho U_0^2 \ell^2 & \int_{L_m} [\delta\varphi]_+^- \Big\{ k_m \cos\beta f(\ell k_m \cos\beta \tilde{s}) \sin(\bar{\alpha} - \delta) + \\
& \cos(\alpha - \delta) \left( \lambda_m k_m \cos\beta + \lambda_h \cos\beta \cos\alpha |\tilde{s}| - \frac{\partial\varphi}{\partial n} \right) \Big\} \, d\tilde{s} = 0.
\end{aligned} \tag{4.3}$$

We can choose a $\delta\varphi$ for which $[\delta\varphi]_+^- > 0$ in a small neighbourhood of an arbitrary point on $L_f$ or $L_m$ and $[\delta\varphi]_+^- = 0$ elsewhere (see [6]). Because we can choose this point anywhere on $L_f$ or $L_m$ we find that both expressions between braces in (4.3) have to be zero on the line segments on which they are defined. In order to obtain simple formulae we introduce the functions $\varphi_i(y,z)$, $i = 1, \ldots, 5$, which satisfy $\Delta\varphi_i = 0$ except on $L_f$ and $L_m$. Furthermore they vanish together with their partial derivatives for $y^2 + z^2 \to \infty$ and on $L_f$ and $L_m$ holds

$$\frac{\partial\varphi_1}{\partial n} = \begin{cases} 1 & \text{on } L_f \\ 0 & \text{on } L_m \end{cases}; \quad \frac{\partial\varphi_2}{\partial n} = \begin{cases} 0 & \text{on } L_f \\ 1 & \text{on } L_m \end{cases};$$

$$\frac{\partial\varphi_3}{\partial n} = \begin{cases} m(\tilde{\sigma}) & \text{on } L_f \\ \tilde{s} & \text{on } L_m \end{cases}; \tag{4.4}$$

$$\frac{\partial\varphi_4}{\partial n} = \begin{cases} k_f\, f(\ell k_f \cos\beta\, \tilde{\sigma}) \sin\bar{\alpha} & \text{on } L_f \\ k_m\, f(\ell k_m \cos\beta\, \tilde{\sigma}) \sin\bar{\alpha} & \text{on } L_m \end{cases};$$

$$\frac{\partial\varphi_5}{\partial n} = \begin{cases} k_f\, f(\ell k_f \ \cos\beta\,\widetilde{\sigma})\cos\overline{\alpha} \ \text{ on } L_f \\ k_m\, f(\ell k_m \ \cos\beta\,\widetilde{s})\cos\overline{\alpha} \ \text{ on } L_m \end{cases}$$

By the definition of $\varphi_4$ and $\varphi_5$ on $L_f$ there holds the identity

$$\frac{\partial}{\partial n}(\varphi_4\cos\delta - \varphi_5\sin\delta) = k_f\, f(\ell k_f\cos\beta\,\widetilde{\sigma})\sin(\overline{\alpha}-\delta)$$

(and the analogous identity on $L_m$). We stress that this linear combination of $\varphi_4$ and $\varphi_5$ is *not* a potential function for $\overline{f^*(\overline{z})}$, (3.1), since $\overline{f^*(\overline{z})}$ cannot possess a potential function. It gives, however, the way in which this non-uniform part of the undisturbed wind is felt by the lifting lines and their free-vortex sheets.

The potential $\varphi$ for which (4.3) holds can now be written as a linear combination of $\varphi_i$:

$$\varphi = \cos\beta\{\lambda_f k_f\varphi_1 + \lambda_m k_m\varphi_2 + \lambda_h \cos\alpha\,\varphi_3 + (\varphi_4\cos\delta - \varphi_5\sin\delta)/\cos(\alpha-\delta)\} \tag{4.5}$$

The constants $\lambda_f$, $\lambda_m$ and $\lambda_h$ are found by inserting (4.5) in (3.12) - (3.14) and solving the three resulting linear equations. For this purpose we first define the following quantities which occur in the various integrals over $\varphi_i$ and $\frac{\partial\varphi_j}{\partial n}$, $i, j = 1, \ldots, 5$:

$$\begin{aligned} I_{ijf} &= \int_{L_f} [\varphi_i]_+^- \frac{\partial\varphi_j}{\partial n}\, d\widetilde{\sigma}, \qquad i, j = 1, \ldots, 5, \\ I_{klm} &= \int_{L_m} [\varphi_k]_+^- \frac{\partial\varphi_l}{\partial n}\, d\widetilde{s}, \qquad k, l = 1, \ldots, 5, \\ I_{pq} &= \int_{L_f} [\varphi_p]_+^- \frac{\partial\varphi_q}{\partial n}\, d\widetilde{\sigma} + \int_{L_m} [\varphi_p]_+^- \frac{\partial\varphi_q}{\partial n}\, d\widetilde{s}, \quad p, q = 3, 4, 5. \end{aligned} \tag{4.6}$$

By the properties of the potential functions $\varphi_i$, (4.4), we find that $I_{i2f} = I_{i1m} = 0$ $(i = 1, \ldots, 5)$. Furthermore, by using Green's second formula and $\Delta\varphi_i = 0$ we can derive several relations between these quantities, which will be used henceforth. For example we find

$$I_{21f} = \int_{L_f} [\varphi_2]_+^- \frac{\partial\varphi_1}{\partial n} = \int_{L_f + L_m} [\varphi_2]_+^- \frac{\partial\varphi_1}{\partial n} = \int_{L_f + L_m} [\varphi_1]_+^- \frac{\partial\varphi_2}{\partial n} = \int_{L_m} [\varphi_1]_+^- \frac{\partial\varphi_2}{\partial n} = I_{12m}.$$

Next we write, still in order to obtain simple formulae, the prescribed sideforces and heeling moment (3.12) - (3.14) as

$$\begin{aligned} F_f &= \rho U_0^2\,\ell^2\cos^2\beta\, k_f\,\mu_f, \quad F_m = \rho U_0^2\,\ell^2\cos^2\beta\, k_m\,\mu_m, \\ M_h &= \rho U_0^2\,\ell^3\cos\beta\,\mu_h\cos\alpha. \end{aligned} \tag{4.7}$$

Here we introduced $\mu_f, \mu_m$ and $\mu_h$ which can be computed when $F_f, F_m$ and $M_h$ are given.

Now (3.12), (3.13) and (3.14) yield the following set of equations for $\lambda_f, \lambda_m$ and $\lambda_h$

$$\begin{pmatrix} I_{11f} & I_{21f} & I_{31f} \\ I_{21f} & I_{22m} & I_{32m} \\ I_{31f} & I_{32m} & I_{33} \end{pmatrix} \begin{pmatrix} \lambda_f k_f \\ \lambda_m k_m \\ \lambda_h \cos\alpha \end{pmatrix} = \begin{pmatrix} \mu_f \\ \mu_m \\ \mu_h \end{pmatrix} - \frac{\cos\delta}{\cos(\alpha-\delta)} \begin{pmatrix} I_{41f} \\ I_{42m} \\ I_{43} \end{pmatrix} + \frac{\sin\delta}{\sin(\alpha-\delta)} \begin{pmatrix} I_{51f} \\ I_{52m} \\ I_{53} \end{pmatrix} \tag{4.8}$$

We can solve these equations and insert the result in the expression for $\varphi$, (4.5), which then becomes a function of $\mu_f, \mu_m$ and $\mu_h$. With this $\varphi$ we find for the induced resistance $R_i$, (3.9):

$$\begin{aligned} R_i = \tfrac{1}{2}\rho U_0^2 \ell^2 \cos^2\beta \{ & c_{ff}\mu_f^2 + c_{mm}\mu_m^2 + c_{hh}\mu_h^2 + 2c_{fm}\mu_f\mu_m + 2c_{fh}\mu_f\mu_h + \\ & 2c_{mh}\mu_m\mu_h + (c_1\cos^2\delta - c_2\sin\delta\cos\delta + c_3\sin^2\delta)/\cos^2(\alpha-\delta)\} \cdot \det{}^{-1} \end{aligned} \tag{4.9}$$

where

$$c_{ff} = I_{22m} I_{33} - I_{32m}^2, \quad c_{mm} - I_{11f} I_{33} - I_{31f}^2, \quad c_{hh} = I_{11f} I_{22m} - I_{21f}^2,$$

$$c_{fm} = I_{31f} I_{32m} - I_{21f} I_{33}, \quad c_{fh} = I_{21f} I_{32m} - I_{31f} I_{22m}, \quad c_{mh} = I_{21f} I_{31f} - I_{11f} I_{32m},$$

$$\det = \begin{vmatrix} I_{11f} & I_{21f} & I_{31f} \\ I_{21f} & I_{22m} & I_{32m} \\ I_{31f} & I_{32m} & I_{33} \end{vmatrix},$$

$$c_1 = I_{44}\det - I_{41f} A_{1s} - I_{42m} A_{2s} - I_{43} A_{3s},$$

$$c_2 = 2I_{45}\det - I_{41f} A_{1c} - I_{42m} A_{2c} - I_{43} A_{3c} - I_{51f} A_{1s} - I_{52m} A_{2s} - I_{53} A_{3c},$$

$$c_3 = I_{55}\det - I_{51f} A_{1c} - I_{52m} A_{2c} - I_{53} A_{3c},$$

$$A_{1s} = \begin{vmatrix} I_{41f} & I_{21f} & I_{31f} \\ I_{42m} & I_{22m} & I_{32m} \\ I_{43} & I_{32m} & I_{33} \end{vmatrix}, \quad A_{1c} = \begin{vmatrix} I_{51f} & I_{21f} & I_{31f} \\ I_{52m} & I_{22m} & I_{32m} \\ I_{53} & I_{32m} & I_{33} \end{vmatrix},$$

$$A_{2s} = \begin{vmatrix} I_{11f} & I_{41f} & I_{31f} \\ I_{21f} & I_{42m} & I_{32m} \\ I_{31f} & I_{43} & I_{33} \end{vmatrix}, \quad A_{2c} = \begin{vmatrix} I_{11f} & I_{51f} & I_{31f} \\ I_{21f} & I_{52m} & I_{32m} \\ I_{31f} & I_{53} & I_{33} \end{vmatrix},$$

$$A_{3s} = \begin{vmatrix} I_{11f} & I_{21f} & I_{41f} \\ I_{21f} & I_{22m} & I_{42m} \\ I_{31f} & I_{32m} & I_{43} \end{vmatrix}, \quad A_{3c} = \begin{vmatrix} I_{11f} & I_{21f} & I_{51f} \\ I_{21f} & I_{22m} & I_{52m} \\ I_{31f} & I_{32m} & I_{53} \end{vmatrix}. \tag{4.10}$$

We observe that the induced resistance is a quadratic function of the prescribed sideforces and heeling moment and that the influence of the non-uniform part of the undisturbed wind is only present in the term which does not depend on $\mu_f, \mu_m$ or $\mu_h$.

The $O(\epsilon^2)$ contribution to the thrust due to the motion of the lifting lines through the $O(\epsilon)$ part of the apparent wind becomes, using (4.5), (4.8) and (3.10):

$$\begin{aligned} &K_x \cos(\alpha - \delta) + K_y \sin(\alpha - \delta) = \\ &\rho U_0^2 \ell^2 \cos^2 \beta \det{}^{-1} \{\cos\delta\, (\mu_f A_{1s} + \mu_m A_{2s} + \mu_h A_{3s}\} - \\ &\qquad \sin\delta\, (\mu_f A_{1c} + \mu_m A_{2c} + \mu_h A_{3c}\} + \\ &\qquad (c_1 \cos^2\delta - c_2 \sin\delta\cos\delta + c_3 \sin^2\delta)/\cos(\alpha - \delta)\} \end{aligned} \tag{4.11}$$

where the various constants are already defined in (4.10).

We remark that all terms in (4.9) and (4.11) are $O(\epsilon^2)$, as they should be. $F_f$, $F_m$ and $M_h$ are $O(\epsilon)$, hence by definition (4.7), $\mu_f$, $\mu_m$ and $\mu_h$ are $O(\epsilon)$. Furthermore $\overline{f^*(\bar{z})}$, (3.1), is assumed to be $O(\epsilon)$. Therefore $\varphi_4$ and $\varphi_5$, (4.4), are $O(\epsilon)$, from which it follows that $A_{is}$ and $A_{ic}$, (4.10), are $O(\epsilon)$ and $c_i$, (4.10), are $O(\epsilon^2)$.

Finally the optimum circulation distribution of fore- and mainsail, $\Gamma_f$ and $\Gamma_m$ respectively, as function of the length parameters $\sigma$ and $s$ (Fig. 3.2) are

$$\Gamma_f(\sigma) = U_0 \ell\, [\varphi(k_f\, \sigma)]_+^- , \tag{4.12}$$

$$\Gamma_m(s) = U_0 \ell\, [\varphi(k_m s)]_+^- . \tag{4.13}$$

Here $\varphi$ is the optimum potential function (4.5), and the jump $[\varphi]_+^-$ is calculated over the free-vortex sheets of fore- and mainsail respectively.

From (4.5) we see that when all parameters and variables have been fixed, apart from the sideforces and the heeling moment, the optimum potential $\varphi$ is a linear combination of only the 5 functions $\varphi_i$, defined in (4.4). Hence also the optimum circulation distribution $\Gamma_f$, (4.12), and $\Gamma_m$, (4.13), can be written as linear combinations of the 5 circulation distributions which belong to $\varphi_i$. The coefficients of the $\varphi_i$ are functionals of the $\varphi_i$ themselves and they depend linearly on the applied sideforces and heeling moment (4.7) as can be seen from (4.8).

## 5. The formulae for the underwatership and the coupling of the two systems

The optimization problem for the underwatership is a rather simple special case of that for the sails. The leeway angle $\lambda$ between $C_L$ and the uniform water velocity $V$ (Fig. 1.1) is assumed to be of $O(\epsilon)$, so in a linearized theory we cannot distinguish between the free-vortex sheets shed by the keel and a separate rudder. Therefore it is meaningless in the optimization problem to prescribe separately the sideforces experienced by keel and rudder, and we can represent the underwatership by one lifting line which terminates at the watersurface. Here we will give only the optimum formulae, a detailed description of the optimization problem can be found e.g. in [6].

Velocities are nondimensionalized by $V$ and lengths by $\ell^w$, which is the depth of the keel. The sideforce $F_w$ is prescribed perpendicular to $C_L$ and the heeling moment $M_h$ is around $C_L$. They are written as

$$F_w = \rho V^2 {\ell^w}^2 \cos^2\beta\, \mu_w, \quad M_h = \rho V^2 {\ell^w}^3 \cos\beta\, \mu_h. \tag{5.1}$$

Then we find for the mimimum induced resistance $R_i$, which acts parallel to $C_L$ and hence, in our linearized theory, in the direction of $V$ (Fig. 1.1):

$$R_i = \tfrac{1}{2}\rho V^2 {\ell^w}^2 \cos^2\beta\, (\mu_w^2 I_{22w} - 2\mu_w\mu_h I_{21w} + {\mu_h}^2 I_{11w})/(I_{11w} I_{22w} - I_{21w}^2). \tag{5.2}$$

The quantities $I_{ijw}$ $(i, j = 1,2)$ are defined in the same way as those in definition (4.6). In fact there holds $I_{ijw} = I_{ijm}$ $(i, j = 1,2)$ when in the case of the sails the foresail is absent and the mainsail extends from the watersurface to the top of the mast.

Now we consider the propulsion unit, consisting of the two coupled systems of lifting surfaces in the air and the water. In Fig. 5.1 the relevant forces and moments are drawn in a coordinate system $X, Y$ fixed to the yacht.

Where confusion can arise we give quantities a superscript $^a$ or $^w$, depending on whether they belong to the air or the water, respectively.

The undisturbed water velocity $V$ makes an angle $\lambda$ of $O(\epsilon)$ with the $X$-axis. The $O(\epsilon^0)$ part $U_0$, (3.2), makes an angle $\alpha$, (3.3), of $O(\epsilon^0)$ with the $X$-axis. The direction in which we want to optimize the thrust makes an angle $\delta$ with the $X$-axis.

Perpendicular to this direction the resultant 'sideforce' must be zero up to and including $O(\epsilon)$. With (4.7) and (5.1) this yields

$$\rho^a U_0^2 {\ell^a}^2 \cos^2\beta\, (\mu_f k_f + \mu_m k_m)\cos(\alpha - \delta) = \rho^w V^2 {\ell^w}^2 \cos^2\beta \mu_w \cos\delta. \tag{5.3}$$

The righting moment $M_r$ is mainly determined by the form of the hull and the distribution of the weight in the keel. It is assumed that it can be written as a function of the heeling angle $\beta$ only:

$$M_r(\beta) = \rho^w V^2 {\ell^w}^3 m(\beta) \tag{5.4}$$

where $m(\beta)$ is a given function.

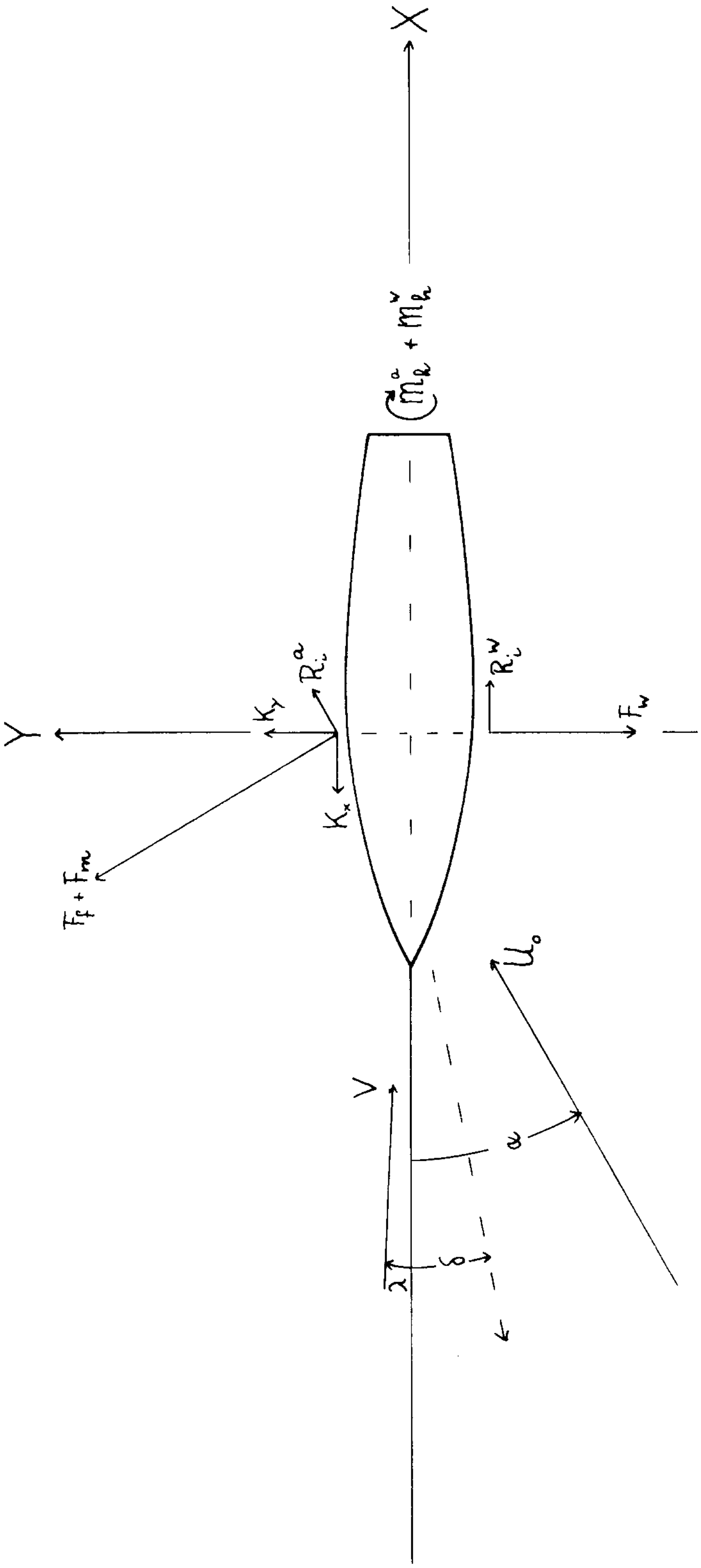


Fig. 5.1 Forces and moments occurring in the optimization problem.

This righting moment must balance the heeling moment of $O(\epsilon)$, exerted on the sails and the keel. With (4.7), (5.1) and (5.4) we find

$$\rho^a U_0^2 \ell^{a^3} \cos\beta \cos\alpha\, \mu_h{}^a + \rho\, w\, V^2\, \ell^{w^3} \cos\beta\, \mu_h{}^w = \rho^w\, V^2\, \ell^{w^3}\, m(\beta). \tag{5.5}$$

The $O(\epsilon^2)$ part of the thrust about which we have information, called $T(\epsilon^2)$, is composed of the forces $K_x$ and $K_y$, (3.10), which are due to the nonuniformity of the undisturbed wind, and the induced resistances of the sails $R_i{}^a$ and the underwatership $R_i{}^w$. In the optimum case $T(\epsilon^2)$ follows from (4.11), (4.9) and (5.2):

$$T(\epsilon^2) = K_x \cos(\alpha - \delta) + K_y \sin(\alpha - \delta) - R_i{}^a \cos(\alpha - \delta) - R_i{}^w \cos\delta. \tag{5.6}$$

Now $\mu_w$ and $\mu_h{}^w$ can be solved from (5.3) and (5.5). We insert them in (5.6) and there remains for $T(\epsilon^2)$ a function of $\mu_f$, $\mu_m$ and $\mu_h{}^a$.

The $O(\epsilon)$ part of the thrust $T(\epsilon)$ is with (4.7) and (5.1):

$$T(\epsilon) = \rho^a U_0^2 \ell^{a^2} \cos^2\beta(\mu_f k_f + \mu_m k_m)\sin(\alpha - \delta) + \rho^w V^2 \ell^{w^2} \cos^2\beta\mu_w \sin\delta. \tag{5.7}$$

Perpendicular to $T$ there remains, again apart from an unknown contribution, which is discussed in Section 2, a sideforce of $O(\epsilon^2)$, called $F(\epsilon^2)$, which is positive in positive $Y$-direction:

$$F(\epsilon^2) = K_y \cos(\alpha - \delta) - K_x \sin(\alpha - \delta) + R_i{}^a \sin(\alpha - \delta) - R_i{}^w \sin\delta. \tag{5.8}$$

We remark that in our mathematical model the two systems of lifting surfaces can only influence one another by the sideforce and heeling moment they generate. This is due to the reduction of the watersurface to a rigid and flat interface between the two media. Then a variation in the circulation distribution of the underwatership, which leaves the sideforce and heeling moment unchanged, is not felt by the sails, and vice versa. If the watersurface had been treated as a free surface such a variation would change the shape of the watersurface, which then would be felt by the circulation distribution of the other system. For this reason we can optimize the sails and the underwatership separately and couple them afterwards by the requirements of zero sideforce (5.3) and zero heeling moment (5.5).

## 6. Numerical results

We will apply our formulae to the yacht which has also been investigated in [8]. The height of the mast, $\ell^a$, is 12 m and the depth of the keel, $\ell^w$, 1.7 m. Its righting moment $M_r(\beta)$, (5.4), is 3400 sin $\beta$ kg m.

The true wind will have a velocity of 9 m/s at a height of 10 m, which corresponds with force 5 on Beaufort's scale. Wieghardt [7] shows that for this wind force a good approximation for the wind profile $U(\bar{z})$, (3.1), is

$$U(\bar{z}) = U(10) \cdot \left(\frac{\bar{z}}{10}\right)^{\frac{1}{10}} = 9\left(\frac{\bar{z}}{10}\right)^{\frac{1}{10}} \text{ m/s}. \tag{6.1}$$

The subdivision of this velocity profile in a uniform part of $O(\epsilon^0)$ plus a part of $O(\epsilon)$ is rather arbitrary. To get an idea of what we call velocities of $O(\epsilon)$ consider a chordwise sail (section) with camber ratio of 0.10. Placed in an apparent wind of say 9 m/s it will feel normal velocities up to 2 - 2.5 m/s, which we have to consider as being of order $\epsilon$ when we want to use linearized lifting-surface theory. Now we can make various choices for $U_0^*$, (3.1), and hence for $\bar{f}^*(\bar{z})$. The choice will influence among other things $U_0$, (3.2), $\alpha$, (3.3), $k_f$ and $k_m$, (3.11), the functions $\varphi_i$, (4.4), and the quantities $\mu_f, \mu_m$ and $\mu_h$, (4.7), when $F_f$, $F_m$ and $M_h$ are given. Obvious values for $U_0^*$ are $U(\bar{1})$, $U(\overline{12})$ or the average of $U(\bar{z})$ over 12 metres (i.e. the height of the mast). Then $U_0^*$ and $\bar{f}^*(\bar{z})$ are respectively

$$\begin{aligned}
&(a)\quad U_0^* = 7.15, \quad \bar{f}^*(\bar{z}) = 9\left(\frac{\bar{z}}{10}\right)^{\frac{1}{10}} - 7.15,\\
&(b)\quad U_0^* = 9.17, \quad \bar{f}^*(\bar{z}) = 9\left(\frac{\bar{z}}{10}\right)^{\frac{1}{10}} - 9.17,\\
&(c)\quad U_0^* = 8.33, \quad \bar{f}^*(\bar{z}) = 9\left(\frac{\bar{z}}{10}\right)^{\frac{1}{10}} - 8.33.
\end{aligned} \tag{6.2}$$

In (6.2c) $\bar{f}^*(\bar{z})$ is negative in the whole range of interest, whereas in (6.2a) it is positive from $\bar{z} = 1$ m. We will compute for these three values of $U_0^*$ the optimum contribution by the sails to $T(\epsilon^2)$, (5.6), when the yacht heels over an angle $\beta = 15°$, and $\bar{\alpha}^*$ (Fig. 3.1) is 60°.

Before giving the numerical results we want to discuss the consequences of the choice of $U_0^*$ in some detail. Suppose the sideforce and heeling moment of the underwatership are given and we take for $U_0^*$ the value 7.15 m/s, (6.2a). Then we calculate the optimum $\varphi$, (4.5), satisfying (5.3) and (5.5), and we find the optimum circulation distributions of the sails $\Gamma_f$ and $\Gamma_m$, which are given in (4.12) and (4.13). Next we construct sails which will have these spanwise circulation distributions, and we place them in the wind profile $U(\bar{z})$, (6.1).

If now we describe the wind by a $U_0^*$ which is for example 9.17 (6.2b) instead of 7.15 these sails would experience a first-order sideforce which is too large by a factor $(U_0\ (1917)/U_0\ (7.15))^2$ if $U_0(\cdot)$ is the apparent wind velocity (3.2), and hence the first-order balance equation (5.3) is violated. The surplus of sideforce, however, is of order $\epsilon^2$, since by assumption the difference between 9.17 m/s and 7.15 m/s if of order $\epsilon$. We tacidly used already the fact that the difference in the apparent wind angles $\alpha$(3.3) is also $O(\epsilon)$. Furthermore we observe that when $U_0^*$ is 7.15 m/s, $\bar{f}^*(\bar{z})$ is positive over most of the span and hence it will yield a positive contribution of order $\epsilon^2$ to the sideforce (5.8). On the other hand for $U_0^* = 9.17$ m/s, $\bar{f}^*(\bar{z})$ is negative everywhere along the span, so it will yield a negative contribution of $O(\epsilon^2)$ to the sideforce which counteracts the aforementioned surplus. The same reasoning holds for the heeling moment. Concluding we remark that the difference in the spanwise circulation distributions belonging to the various values of $U_0^*$ are of order $\epsilon^2$.

In order to obtain sideforces and moments with realistic values we consider until further notice the underwatership as a lifting surface which approximates the projection of keel plus hull on the longitudinal centre plane of the yacht (Fig. 6.1a). (In [8] this underwatership is called A II).

Hence we do not use an optimum underwatership, as is done in Section 5. Of course the balance equations (5.3) and (5.5) must be satisfied, however, now $\mu_w$ and $\mu_h{}^w$ are determined by the shape of the underwatership. Then sideforce $L$, heeling moment $M$ and induced resistance $D$ of

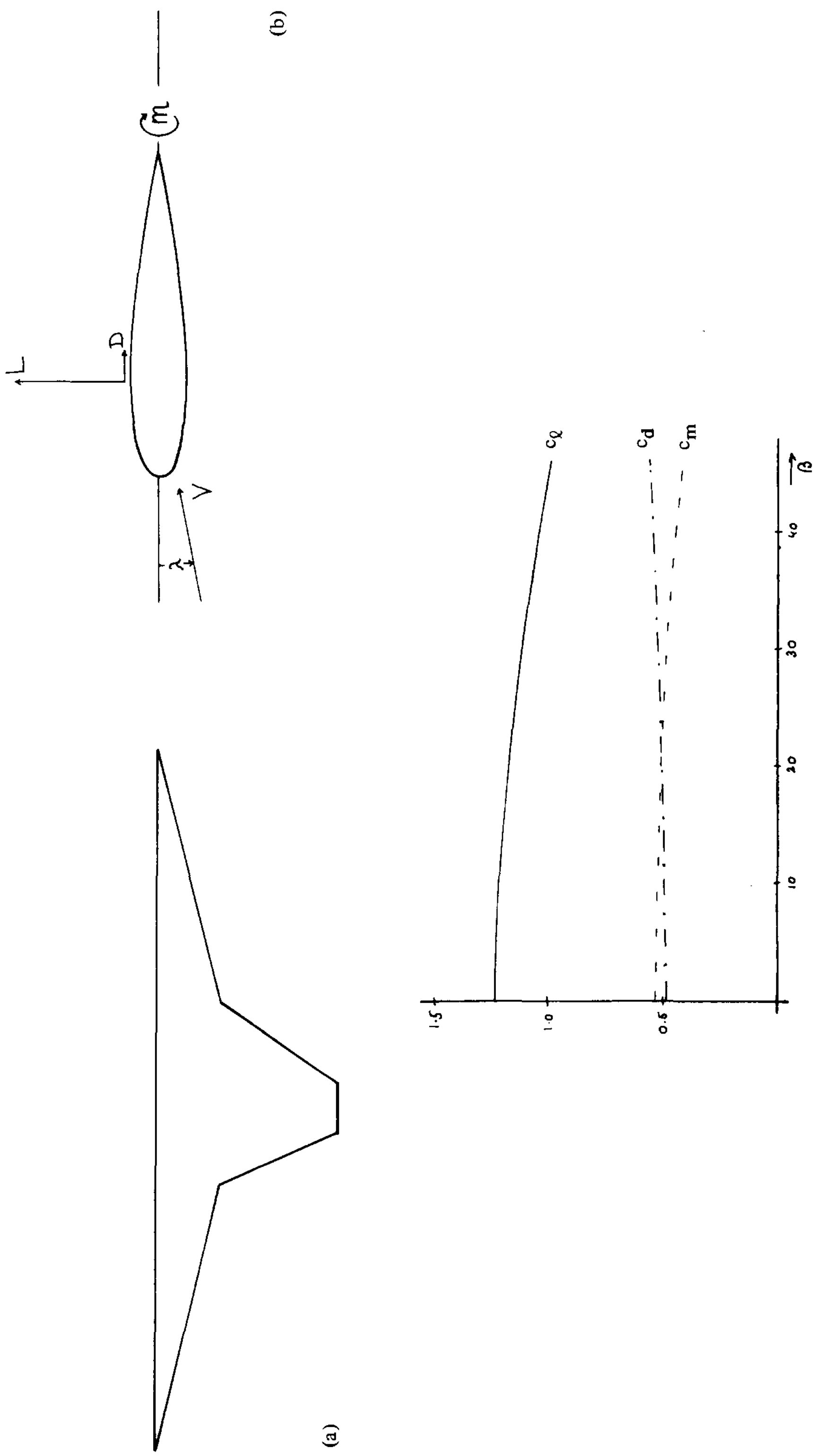


Fig. 6.1 (a) Lifting surface approximating the underwatership.
(b) Positive directions of L, M and D.
(c) $c_\ell$, $c_m$ and $c_d$ as functions of $\beta$.

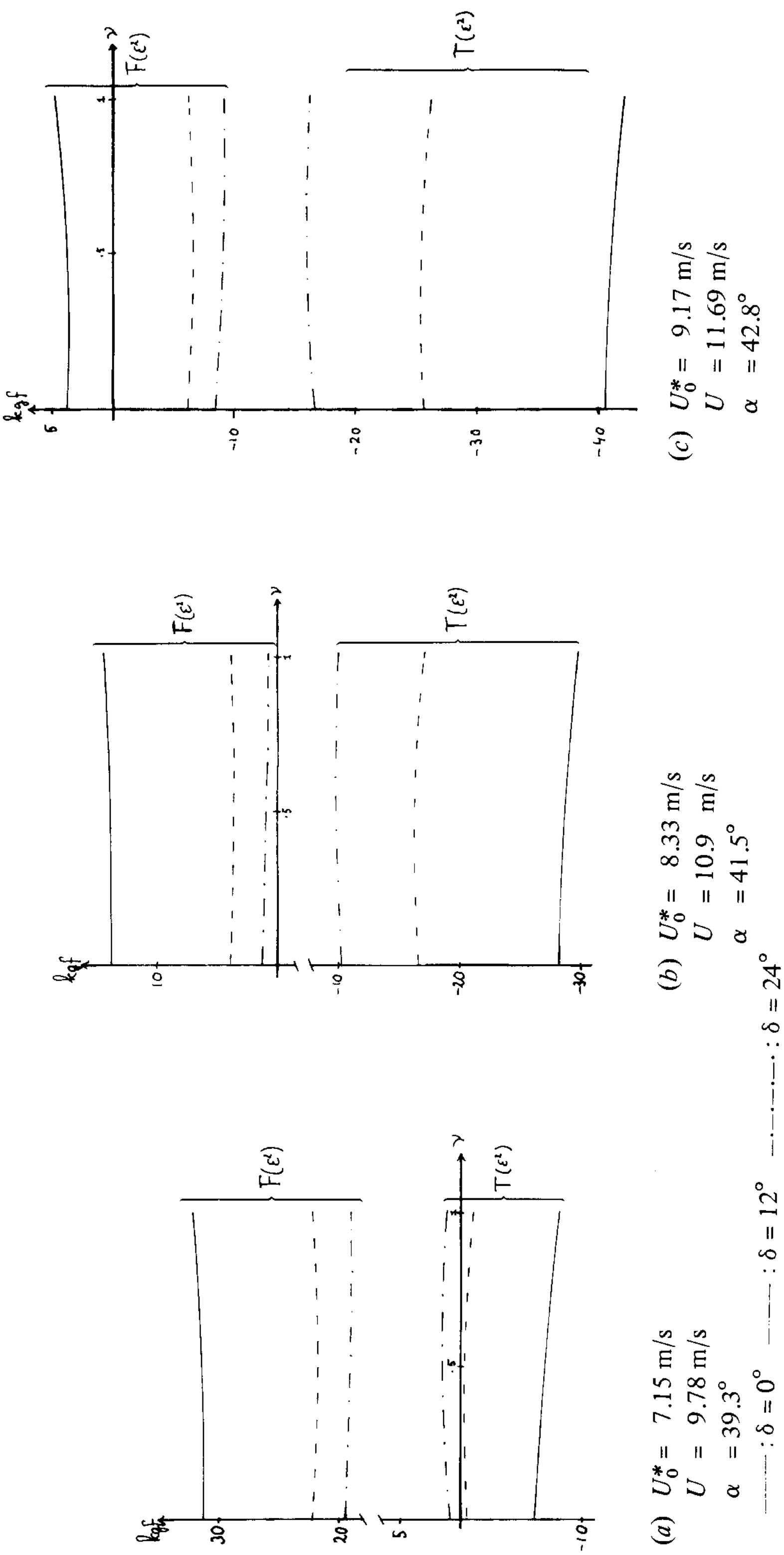


Fig. 6.2 $O(\epsilon^2)$ contributions of sails to thrust and sideforce.
$\overline{\alpha}^* = 60°$, $\beta = 15°$, $V = 4$ m/s, $\lambda = 2°$.

the underwatership (Fig. 6.1b) can be calculated as functions of $\beta$ and $\lambda$, the leeway angle. We introduce lift-, moment- and drag coefficient for the underwatership, $c_\ell, c_m$ and $c_d$, respectively,

$$L = \rho^w V^2 \ell^{w^2} \cos^2 \beta \lambda c_\ell, \quad M = \rho^w V^2 \ell^{w^3} \cos \beta \lambda c_m, \quad D = \rho^w V^2 \ell^{w^2} \cos^2 \beta \lambda^2 c_d. \tag{6.3}$$

These coefficients are still functions of the heeling angle $\beta$. Their dependence on $\beta$ is given in Fig. 6.1c.

Another approach would be to use experimental data for $L$, $M$ and $D$ as functions of $\beta$ and $\lambda$, however, we do not have these at our disposal.

Now for $\beta = 15^\circ$ we find from Fig. 6.1c $c_\ell = 1.204$ and $c_m = 0.516$, hence in the balance equations (5.3) and (5.5) we have to substitute $\mu_w = 1.204\ \lambda$ and $\mu_h^w = 0.516\ \lambda$. The lifting lines representing the fore- and mainsail extend from $\sigma_C = 0.02\ |ET|$ to $\sigma_D = 0.98\ |ET|$ and from $s_A = 0.05\ |OT|$ to $s_B = 0.98\ |OT|$ respectively (Fig. 3.2). The dimensionless distance of the foot of the mast to the point of attachment of the forestay at the deck $e$, (3.7), is 0.3.

Finally we have to fix values for $V$ and $\lambda$. In the real sailing world these are interwoven with each other, with $U(\bar{z})$, the yacht's resistance etc., but we simply choose $V = 4$ m/s and $\lambda = 2^\circ$. In Fig. 6.2 we give the $O(\epsilon^2)$ contributions of the sails to the thrust (5.6) and the sideforce (5.8) for the three values of $U_0^*$ in (6.1). The computations are performed for three values of $\delta$, the angle between $C_L$ and the thrust. On the horizontal axis we have plotted the quotient $\nu = F_m/F_f$ which gives the ratio of the sideforces exerted by main- and foresail; $\nu$ ranges from 0 to 1.

We see that for $\delta = 0^\circ$, i.e. thrust parallel to the yacht's centreline, $T(\epsilon^2)$ is a slightly decreasing function of $\nu$ and for $\delta = 12^\circ$ or $\delta = 24^\circ$ it has a weak maximum on the interval $0 \leq \nu \leq 1$. The variations, however, are small. This is not unfavourable, since it is a well-known fact that in the case of interacting sails the lift of the foresail tends to increase at the cost of the lift experienced by the mainsail. Hence we can distribute the sideforce over fore- and mainsail in a realistic way without too ill effects for the second-order thrust. Fig. 6.3 shows the spanwise circulation distributions $\Gamma/\ell$, (4.12, 4.13), for $\delta = 12^\circ$, $\nu = 0{,}6$ and the three values of $U_0^*$, (6.2a - 6.2c). The circulation is calculated along contours in planes perpendicular to the mast as will always be done. We see that the graphs are roughly similar. In the following calculations we will choose $U_0^* = 8.33$ m/s.

From Fig. 6.4 it follows that, although $T(\epsilon^2)$ depends only weakly on $\nu$ (the ratio of $F_m$ and $F_f$), the spanwise circulation distributions $\Gamma/U_0\ell$ of fore- and mainsail vary strongly with $\nu$. We observe that for $\nu \lesssim 0.6$ the circulation of the mainsail becomes negative near the top of the mast. This implies negative pressure differences over the sail, which it can only withstand by a 'negative' curvature. These situations, however, should be avoided because the appropriate sailforms may be expected to be rather unstable. Moreover where the circulation of the mainsail is negative that of the foresail must be extra positive which requires a large camber near the top of the sail, which enlarges the chance of flow separation. We emphasize, however, that these graphs show that 'backwinding' of the mainsail is not necessarily harmful for the performance of a sailing yacht.

Not only with a fore- and mainsail of comparable span, but also when the span of the mainsail is considerably smaller than that of the foresail, the second-order thrust is rather independent of $\nu$. Moreover, given a required sideforce and heeling moment, the dependence of the second-order thrust on the span of the mainsail is small. This is shown in Fig. 6.5, where we give the dependence of $T(\epsilon^2)$ on the angle $\delta$, still with the same choice of the parameters only for dif-

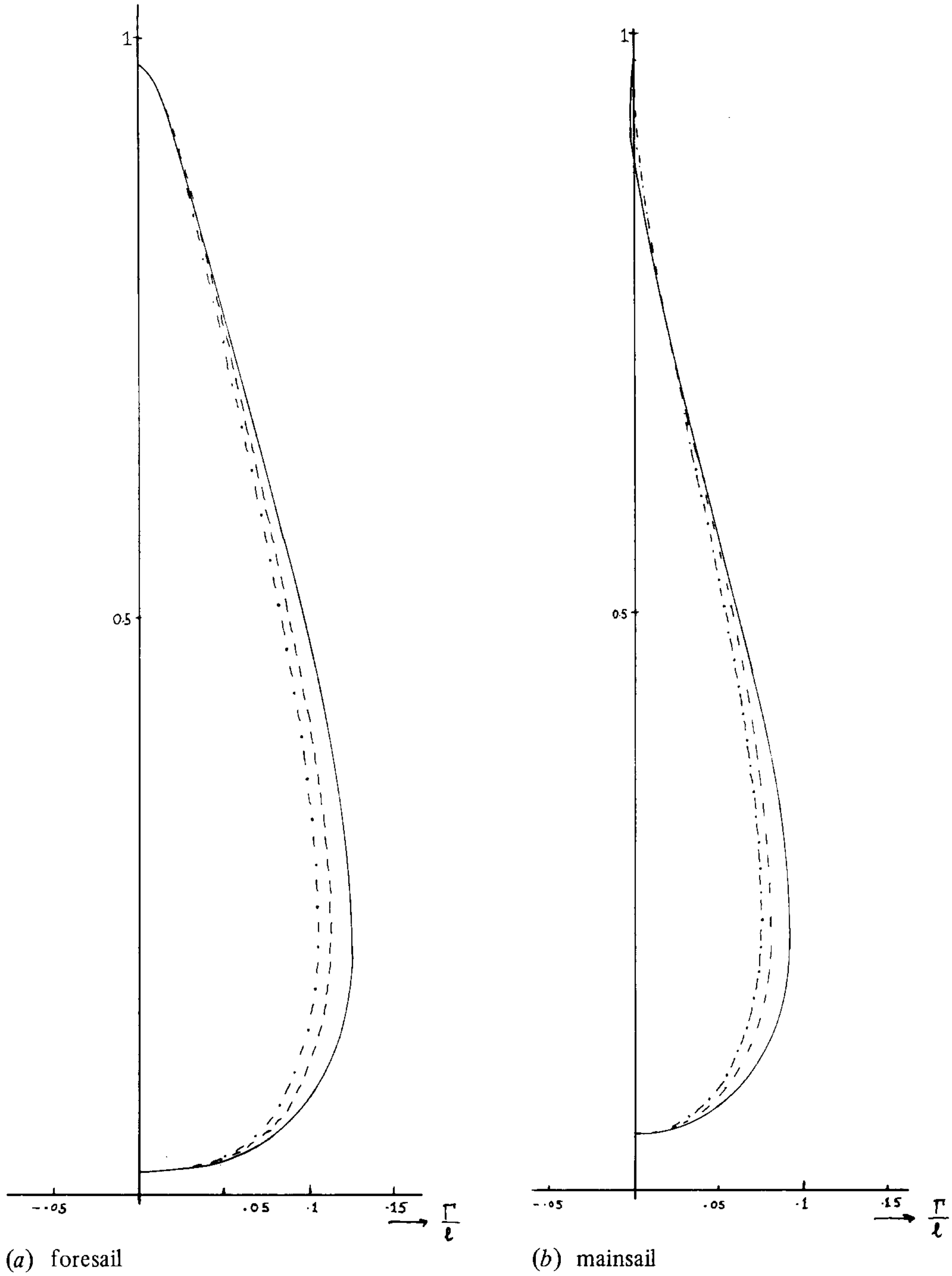


—— : $U_0^* = 7.15$ m/s ------ : $U_0^* = 8.33$ m/s -·-·-·- : $U_0^* = 9.17$ m/s

Fig. 6.3 Circulation distributions of fore- and mainsail as functions of distance to the watersurface $\beta = 15°$, $\bar{\alpha}^* = 60°$, $\delta = 12°$, $\nu = 0.6$.

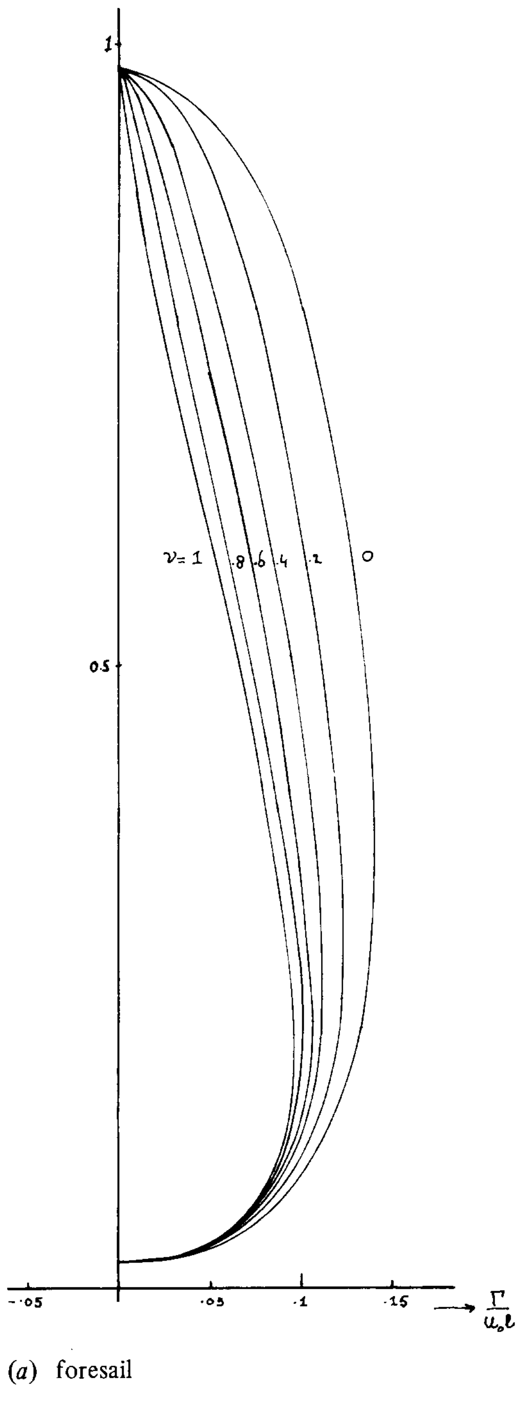


(*a*) foresail

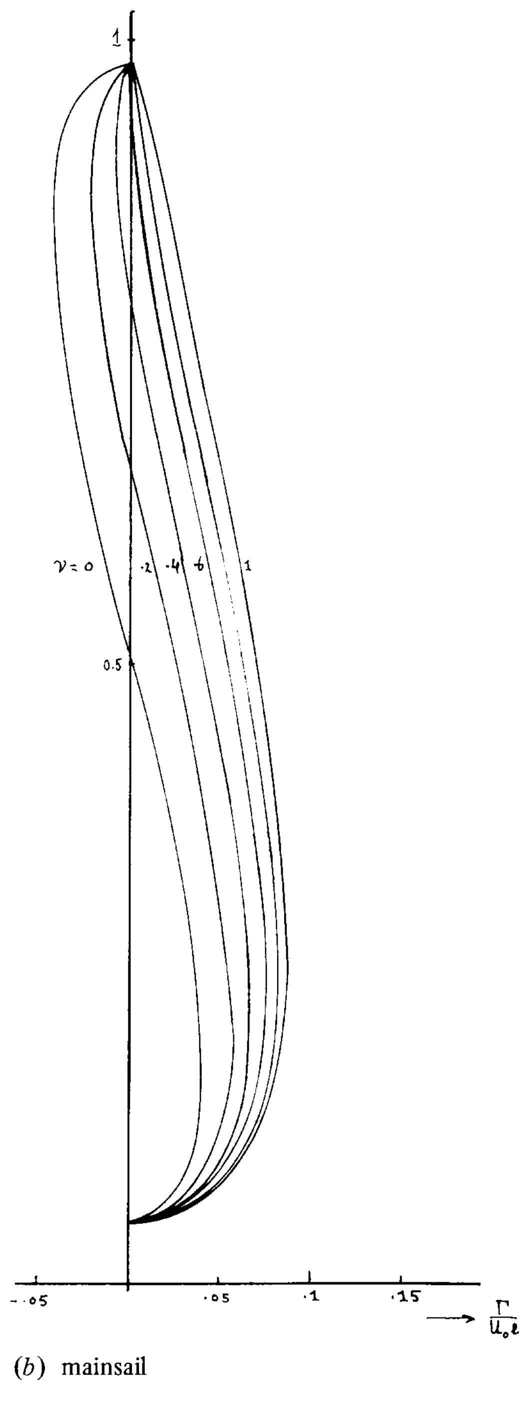


(*b*) mainsail

Fig. 6.4 Dependence of circulation distributions on $\nu$. $\beta = 15°$, $\bar{\alpha}^* = 60°$, $\delta = 12°$, $\lambda = 2°$, V = 4 m/s.

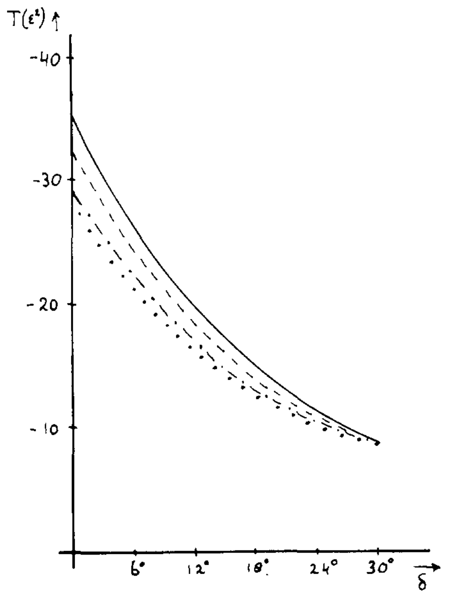


––– : foresail only ; —— : mainsail only

–·–·– : $s_b = 0.8\ |OT|$ ; . . . . .: $s_b = 0.6\ |OT|$

Fig. 6.5 Dependence of T($\epsilon^2$) on the span of fore- and mainsail.

ferent lengths of the mainsail. For $s_A = 0.05\ |OT|$, $s_B = 0.8\ |OT|$ we take $\nu = 0.6$ and for $s_A = 0.05\ |OT|$, $s_B = 0.6\ |OT|$, $\nu$ is 0.4. The graph for $s_A = 0.05\ |OT|$, $s_B = 0.98\ |OT|$, $\nu = 0.8$ is not drawn since it differs only 3 - 4% from the one of $s_B = 0.8\ |OT|$ etc. Now the question arises whether there will be much difference between the second-order thrust of two sails and of one sail with the same effective span. By effective span we mean the span of one sail, whose projected area on the $X,Z$-plane covers the projected areas of fore- and mainsail on the $X,Z$-plane. This concept appears useful, because it leaves intact the interval in $z$-direction which is filled up with free vortices and also the smallest gap between sails and water surface. This gap is very important as has been shown in [6]. Therefore in Fig. 6.5 we also give the graphs for one foresail, $\sigma_C = 0.02\ |ET|$ $\sigma_D = 0.98\ |ET|$ and one mainsail, $s_A = 0.02\ |OT|$ $s_B = 0.98\ |OT|$, separately. We observe that a combination of two sails is slightly better than one fore- or mainsail with the same side force and heeling moment. The superiority of one foresail over one mainsail can be explained by the fact that it is 'less heeled' (Fig. 3.3) so that it has more freedom with respect to the constraint on the heeling moment.

Next we consider the dependence of the heeling moment on $\nu$ where only constraints are imposed on the two sideforces $F_f$ and $F_m$. Then in the optimization problem of Section 4 we have to ignore $\lambda_h$, (4.2), and $\mu_h$, (4.7). The potential function $\varphi_3$, (4.4), does not occur and neither do the quantities $I_{ijf}$, $I_{pqm}$, (4.6), in which one of the indices is 3. Now we obtain in a simple way the formulae for the induced resistance $R_i$, (3.9), and the second-order forces $K_x$ and $K_y$, (3.10), by inserting in (4.9), (4.10) and (4.11) $\mu_h = 0$, $I_{31f} = I_{32m} = I_{43} = I_{53} = 0$ and $I_{33} = 1$. By this the influence of the heeling moment on $R_i$, $K_x$ and $K_y$ disappears (as it should), whereas we can still use the solution of the three equations (4.8) for $\lambda_h$, $\lambda_m$ and $\mu_h$, for now the third equation of (4.8) reads $\lambda_h \cos\alpha = 0$. The heeling moment is found by inserting the optimum potential $\varphi$, (4.5), in the expression for the heeling moment (3.14). Once again we consider the set of sails used for Fig. 6.2 with the same leeway angle, heeling angle etc. In Fig. 6.6 the dependence of the heeling moment on $\nu$ is shown for various spans of the mainsail. For $s_B \lesssim 0.8\ |OT|$ the heeling moment is a decreasing function of $\nu$. When reefing the mainsail it is reasonable to let $\nu$ decrease proportional to the area of the mainsail. If, for $s_B = 0.98\ |OT|$, $\nu$ is 0.8 the corresponding positions on the graphs for smaller $s_B$ are marked and we observe that reefing the mainsail is favourable although the sideforce of the foresail has to increase, since the same total sideforce must be produced. We do not give here the optimum second-order thrust. We only remark that it is larger than when also the heeling moment was prescribed, since here the class of allowed functions $\varphi$, (4.5), is greater.

At the end of this section we want to consider the thrust $T(\epsilon^2)$, (5.6), for the case where also the circulation distribution of the underwatership can be chosen freely. We begin by choosing $\nu$, hence the distribution of sideforce over fore- and mainsail is fixed. Next we solve $\mu_f$ and $\mu_h{}^a$ from (5.3) and (5.5) and insert their values in (5.6), by which $T(\epsilon^2)$ becomes a quadratic function of $\mu_w$ and $\mu_h{}^w$. Now we can find the $\mu_w$ and $\mu_h{}^w$ for which $T(\epsilon^2)$ assumes its maximum. When we have fixed the variables which we can fix, i.e. the span and position of the lifting lines, the true wind angle $\bar{\alpha}^*$, the wind profile $U^*(\bar{z})$ and the righting moment $M_r(\beta)$, the so found maximum $T(\epsilon^2)$ still is a function of the yacht's speed $V$, the leeway angle $\lambda$, the heeling angle $\beta$ and $\delta$. The procedure in [8] was to choose $V$ and then find for various values of the apparent wind angle $\alpha$ the $\lambda$ and $\beta$ which yield maximum thrust. This thrust was compared with the thrust obtained when optimum sails are coupled with an underwatership of given shape, such as in Fig. 6.1a. Here we will not go through all these computations. We will check whether the second objection made at the end of the Introduction concerning the use of optimizing the second-order thrust is serious. To this end we compute for a special case the $\mu_w$ and $\mu_h{}^w$ which give an optimum $T(\epsilon^2)$ and we examine whether they are realistic. By this we mean that the

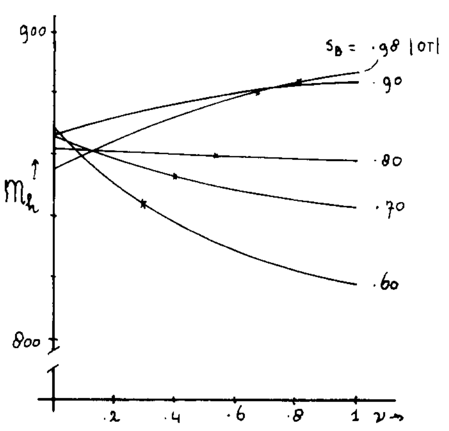


Fig. 6.6 Dependence of heeling moment on and the span of the mainsail. $\delta = 18°$, $\bar{\alpha}^* = 60°$, $\beta = 15°$, $\lambda = 2°$.

connected sideforce and heeling moment are comparable with those which can be generated by an existing underwatership, in our case the one from Fig. 6.1a.

The sails are the ones used for Fig. 6.2, the true wind angle $\bar{\alpha}^*$ is 70°, the yacht's speed $V$ is 4 m/s, the direction of the thrust $\delta$ is 14°, and $\nu$ is 0.6. In Table 6.I we give the optimal $\mu_w$ and $\mu_h{}^w$ for heeling angles $\beta$ ranging from 10° to 35°. Computations show that for leeway angles $\lambda$ between 0° and 4° the variations of these $\mu_w$ and $\mu_h{}^w$ are within 1%. The allied second-order sailforces show variations in the order of 5%. For $\lambda = 3°$ and $\beta = 25°$ we find for this sailforce a value of −29.12 kgf.

| $\beta$ | $\mu_w$ | $\mu_h{}^w$ |
|---|---|---|
| 10° | 0.0188 | 0.0109 |
| 15° | 0.0313 | 0.0148 |
| 20° | 0.0453 | 0.0214 |
| 25° | 0.0613 | 0.0289 |
| 30° | 0.0804 | 0.0379 |
| 35° | 0.1043 | 0.0489 |

TABLE 6.I

| $\lambda$ | $T(\epsilon^2)$ | $\mu_w$ | $\mu_h{}^w$ |
|---|---|---|---|
| 2° | −64.67 | 0.0404 | 0.0173 |
| 2.5° | −40.18 | 0.0505 | 0.0216 |
| 3° | −30.30 | 0.0606 | 0.0259 |
| 3.5° | −35.02 | 0.0708 | 0.0302 |
| 4° | −54.35 | 0.0809 | 0.0345 |

TABLE 6.II

In Table 6.II we have calculated for a set of leeway angles the second-order sailforces of the same yacht in the same position ($\beta = 25°$), only now we used the non-optimum underwatership from Fig. 6.1. The values of $\mu_w$ and $\mu_h{}^w$ for the various values of $\lambda$, which can be deduced from (5.1) and (6.3), are also given. We observe that the maximum $T(\epsilon^2)$ is attained for $\lambda \approx 3°$ and that its value differs about 3% from the optimum value of −29.12 kgf. Furthermore we see that the corresponding $\mu_w$ and $\mu_h{}^w$ are of a magnitude which is comparable with the optimum $\mu_w$ and $\mu_h{}^w$. This means that the mentioned objection can be refuted, i.e. the optimum $\mu_w$ and $\mu_h{}^w$, and hence the optimum sideforce and heeling moment, have values which are compatible with those attained in real sailing situations. So perhaps this theory can be used to gain some driving force by applying slight alternations in the shape of sails and underwatership. On the other hand one can say that the model we used here for the underwatership is almost optimum in the sense of optimality used here.

## 7. The asymptotic case of sailing close to wind

In this section we want to investigate the mathematical validity of the asymptotic theory for sailing close to wind. This theory, which is described in [6], assumes that the true wind angle $\bar{\alpha}^*$ (Fig. 3.1) is $O(\epsilon)$. The consequences of this are the following. The apparent wind angle $\alpha$, (3.3), is $O(\epsilon)$, so that within the accuracy of a linearized theory the $\bar{X}$- and $X$-axis coincide (Figs. 3.1 and 3.2). Therefore the two sails are not distinguishable anymore and we can represent them by one lifting line. From the non-uniform wind (3.6) only the $O(\epsilon)$ part of its $y$-component ($-\lambda V/U_0$) yields a second-order contribution to the thrust $T(\epsilon^2)$, (5.6), because now also the angle $\delta$ (Fig. 5.1) is $O(\epsilon)$. For this reason now the contribution of the sideforce to the thrust in a 'direction' $\delta$, which was $O(\epsilon)$, (5.7), becomes $O(\epsilon^2)$. Hence now the strength of the total driving force is only $O(\epsilon^2)$ and the optimization problem is reduced to finding the maximum second-order thrust of one lifting line, which we locate along the mast, and whose direction of motion makes an angle of $O(\epsilon)$ with the direction of the apparent wind, which now has a uniform velocity profile. If we use the same notations as before and apply the proper linearizations, the asymptotic thrust $T_a(\epsilon^2)$ of the sails in a direction $\delta$ is found from (4.7), (4.9) and (3.10):

$$T_a(\epsilon^2) = F_m(\alpha - \delta) + K_x - R_i^a \tag{7.1}$$

where, as mentioned before, the force $K_x$ is due to the velocity component $-\lambda V/U_0$, and its magnitude is $-\lambda V/U_0 \cdot F_m$. Allowance for $\lambda$ can also be made by reducing the apparent wind angle $\alpha$ with an amount of $-\lambda V/U_0$, as can be seen most easily from formula (7.1). In fact this has been done in [8]. In the present approach we see that the leeway angle causes a resisting force.

The thrust $T_a(\epsilon^2)$ has to be compared with the sum of the first- and second-order contribution by the sails to the thrust. This sum, which we call $T_s$, follows from (4.7), (4.9) and (4.11):

$$T_s = (F_f + F_m)\sin(\alpha - \delta) + K_x \cos(\alpha - \delta) + K_y \sin(\alpha - \delta) - R_i^a \cos(\alpha - \delta). \tag{7.2}$$

We will consider the same pair of sails as in Fig. 6.2 with $\nu = 0.8$. In the asymptotic theory the one lifting line along the mast extends from $s_A = 0.02\ |OT|$ to $s_B = 0.98\ |OT|$, so that it has the same effective span as the two sails. The heeling angle $\beta$ is 15°. The underwatership of Fig. 6.1a is used to fix the constraint on sideforce and heeling moment. The leeway angle $\lambda$ is 2° and $V$ is 3 m/s. Of course it is not realistic to assume that $\lambda$ and $V$ remain constant when the true wind angle $\bar{\alpha}^*$ decreases. It is to be expected that with decreasing $\bar{\alpha}^*$, $V$ will also decrease whereas $\lambda$ increases. Here, however, we want to go into the mathematical, not the physical, validity of the asymptotic theory, so we keep $\lambda$ and $V$ constant throughout the computations. In Fig. 7.1 we show $T_a$ and $T_s$ for $\delta$ = 3°, 9°, 15°, while the true wind angle $\bar{\alpha}^*$ ranges from 20° to 50°. With a boat speed $V$ of 3 m/s the apparent wind angle $\alpha$ (3.3) then ranges from 15° to 37°.

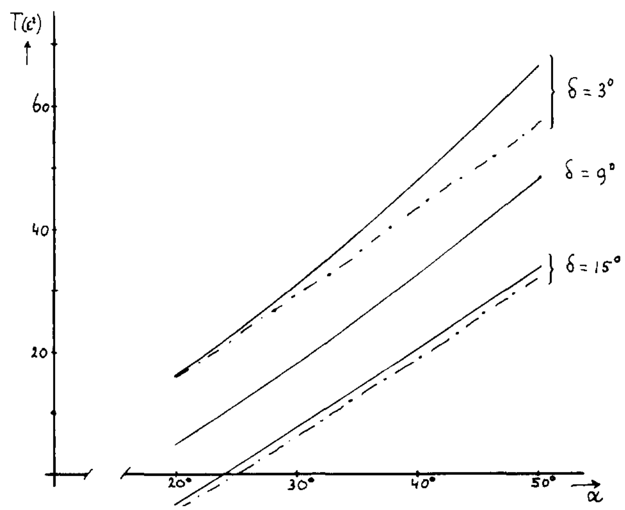


Fig. 7.1 Comparison of asymptotic and 'exact' thrust.

For $\delta = 9^\circ$ the graphs of $T_a$ and $T_s$ differ less than 3%. In general $\delta$ will be greater than $3^\circ$. Then we observe that for $15^\circ \leq \alpha \leq 35^\circ$ the asymptotic theory gives a good prediction of the optimum thrust. Anyway it can be used to study trends such as the influence of the gap between sails deck [6], and the profit of optimizing the circulation distribution of the underwatership [8].

## 8. Concluding remarks

In this paper we consider a sailing yacht as a single propulsion unit consisting of two coupled systems of lifting surfaces with zero thickness. This enables us to use a linearized lifting-surface theory, by which we can calculate some important forces acting on the yacht, i.e. the first-order sideforce, driving force and heeling moment. Inherent in these forces and this moment are forces and moments of second and higher order. Some terms of the second-order quantities can be calculated within the linearized theory we use. The important quantity here is the second-order driving force, since it contributes to the yacht's speed. Therefore we optimized this force under given constaints on the fist-order sideforce and heeling moment. Now our theoretical results could be used as follows.

A yacht with given dimensions, sail area etc, sails to windward in a wind profile $U(\bar{z})$, (3.1), with a thrue wind angle $\bar{\alpha}^*$, (Fig. 3.1). We prescribe its heeling angle $\beta$, where we take into account for example the fact that the wave resistance increases with increasing heeling angle. Then the first-order righting moment is known and hence the heeling moment. Furtermore there are limits to the sideforce (and hence the driving force), for exemple because too large angles of incidence willl cause flow separation. We assume that we know from experience the maximum first-order lift forces which can be generated by sails and underwatership. Due to these forces there exists a leeway angle $\lambda$ of order $\epsilon$ and a yacht's speed $V$ of zeroth order. In general the second-order driving force will not have its maximum value. Then here we can use our optimization theory to enhance the total driving force with more subtle methods than merely increasing the angles of incidence. This larger driving force will cause an increase of $V$, so we have to start an iterative process to find the yacht's final speed. We remark that it seems reasonable to expect an increase of $V$ of order $\epsilon$ since it is only the *second*-order driving force which has changed. So the increase of $V$ has to be added to the first-order apparent wind (3.6).

Until now we have paid no attention to the other second-order quantities. In our theory we have demanded an equilibrium of sideforce and moment up to and including $O(\epsilon)$ ((5.3) and (5.5)). There are left over a sideforce and a moment, both of order $\epsilon^2$, which can cause errors in the prescribed sideforce and heeling moment and in the calculated second-order thrust. As we assume that a sideforce of $O(\epsilon)$ causes a leeway angle $\lambda$ of $O(\epsilon)$ it seems reasonable to expect a leeway angle of order $\epsilon^2$ due to a sideforce of order $\epsilon^2$. Then an error in the sideforce of this order of magnitude has no consequences for the asymptotic accuracy of our theory. A consideration, similar to that for the sideforce, does expect an error in the heeling angle $\beta$ of order $\epsilon$ due to a moment of order $\epsilon^2$. (Here we assumed $\beta$ to be of order $\epsilon^0$). It is easily seen, for example from (3.12) and (3.13), that a change in $\beta$ of order $\epsilon$ yields a change in the sideforce of order $\epsilon^2$. Hence also the thrust will change of order $\epsilon^2$ and this is exactly the order of magnitude within which we perform our optimization. Therefore if we want to apply our theory we have to require that the heeling angle keeps its prescribed value up to and including $O(\epsilon)$. In practice this could be achieved for example by giving the crew the proper positions. The consequences of the uncompensated second-order moment can be bypassed by the theoretical trick of also considering the heeling angle $\beta$ to be of order $\epsilon$. For heeling angles which do not exceed 25° this seems not unrealistic. Then the change in $\beta$ will be of second order and hence the change in the sideforce is of order $\epsilon^3$. We remark however that the assumption in the calculations of a constant heeling angle is of the same nature as the assumption of a constant yacht's speed $V$.

## REFERENCES

[1] H. Ashley & M. Landahl, *Aerodynamics of wings and bodies*, Addison-Wesley Publ. Cy. (1965).
[2] J. Baader, *Zeilsport, zeiltechniek, zeiljachten* (Dutch translation) Hollandia N.V., Baarn, The Netherlands (1965).
[3] C. A. Marchaj, *Sailing theory and practice*, Dodd, Mead & Company, New York (1964).
[4] J. H. Milgram, The analytical design of yacht sails, *Trans. SNAME* 74 (1968) 118-160.
[5] J. A. Sparenberg, Note on the induced drag of sails and keel of a yacht. *Unpublished paper.*
[6] J. A. Sparenberg & A. K. Wiersma, On the maximum thrust of sails by sailing close to wind, *Journal of Ship Research* 20 (1976) 98-106.
[7] K. Wieghardt, Zum Windprofil über See, *Schiffstechnik* 19 (96) (1972) 35-37.
[8] A. K. Wiersma, On the profit of optimizing the fin-keel of a yacht sailing close to wind, *Journal of Engineering Mathematics* 12 (1978) 357-364.
[9] C. J. Wood, & S. H. Tan, Towards an optimum yacht sail, *Journal of Fluid Mechanics* 85 (1978) 459-477.